Late-Transition-Metal Complexes of BINOL-Derived Salens: Synthesis, Structure, and Reactivity

Erin F. DiMauro and Marisa C. Kozlowski*

Department of Chemistry, Roy and Diana Vagelos Laboratories, University of Pennsylvania, Philadelphia, Pennsylvania 19104

Received June 27, 2001

Salen metal complexes incorporating two chiral BINOL moieties have been synthesized. From a comparison of the parent salen and the BINOL−salen X-ray crystal structures, the effect of the BINOL portions has been examined. In particular, the effects of intramolecular hydrogen bonding on the salen core structure have been determined. The bis(naphthoxide) complexes arising from deprotonation of the BINOL−salen metal complexes have been found to catalyze the asymmetric addition of benzyl malonate to cyclohexenone in up to 90% ee.

Introduction

A number of recent studies have shown that multifunctional ligands possess useful characteristics for catalysis and asymmetric synthesis.[1] For example, ligands have been reported in which one portion engages a Lewis acid moiety that coordinates an electrophilic substrate, while another portion of the ligand coordinates to the nucleophilic substrate partner. The positioning by such a catalyst assembly of the two reactant partners in close proximity and with the correct relative geometry facilitates a reaction in a manner similar to that of some enzyme catalysts (i.e., ligases). Dual coordination by such catalyst assemblies further enables the reaction by simultaneously enhancing the electrophilic character of one partner and the nucleophilic character of the other partner.[2]

An example of this motif can be found in the heterobimetallic complexes (**1**) developed by Shibasaki et al. (Figure 1).[1c,d] In these complexes, the central lanthanide metal is proposed to coordinate the electrophile, while the hemilable BINOLate oxygens deprotonate the nucleophile. While several bifunctional ligands that operate along these lines have been discovered,[1,3] relatively few examples exist in which electronically decoupled sites are present for individual activation of the electrophilic and nucleophilic substrates.[4]

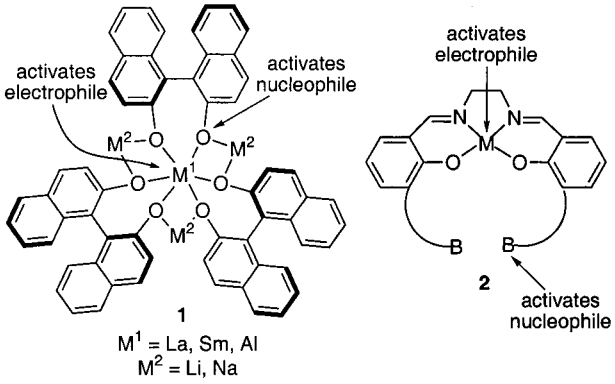

Figure 1.

We have investigated a family of salen metal complexes of the general structure **2** in which Lewis acid and base elements can be independently manipulated (Figure 1).[5] The ease of preparation and derivatization of the structurally well-defined and rigid salen backbone makes this motif an ideal starting point for the construction of a number of such bifunctional ligands. The apical coordination site at the Lewis acidic salen metal center could serve to activate an electrophile. The pendant base could activate a nucleophilic component.

To prevent internal complexation of the base with the salen metal, a short and/or rigid enough tether must be used to connect the salen to the basic functional group. Several types of salens which satisfy these criteria are illustrated in Figure 2. These compounds can be grouped into two different classes according to the type of basic functional group employed. For example, **3** and **4** contain a tertiary amine base, while

(1) (a) Corey, E. J.; Bakshi, R. K.; Shibata, S. *J. Am. Chem. Soc.* **1987**, *109*, 5551−5553. (b) Kitamura, M.; Suga, S.; Niwa, M.; Noyori, R. *J. Am. Chem. Soc.* **1995**, *117*, 4832−4842. (c) Shibasaki, M.; Sasai, H.; Arai, T. *Angew. Chem., Int. Ed. Engl.* **1997**, *36*, 1236−1256. (d) Kim, Y. S.; Matsunaga, S.; Das, J.; Sekine, A.; Oshima, T.; Shibasaki, M. *J. Am. Chem. Soc.* **2000**, *122*, 6506−6507 and references therein. (e) Gample, M. P.; Smith, A. R. C.; Wills, M. *J. Org. Chem.* **1998**, *63*, 6068−6071. (f) Yamakawa, M.; Ito, H.; Noyori, R. *J. Am. Chem. Soc.* **2000**, *122*, 1466−1478 and references therein. (g) Trost, B. M.; Ito, H. *J. Am. Chem. Soc.* **2000**, *122*, 12003−12004. (h) List, B.; Pojarliev, P.; Castello, C. *Org. Lett.* **2001**, *3*, 573−575 and references cited therein.

(2) For reviews on bifunctional catalysis, see: Sawamura, M.; Ito, Y. *Chem. Rev.* **1992**, *92*, 857−871. van den Beuken, E. K.; Feringa, B. L. *Tetrahedron* **1998**, *54*, 12985−13011. Rowlands, G. J. *Tetrahedron* **2001**, *57*, 1865−1882.

(3) For other bimetallic catalysts, see the following. Al·Li: (a) Keller, E.; Veldman, N.; Spek, A. L.; Feringa, B. L. *Tetrahedron: Asymmetry* **1997**, *8*, 3403−3413. (b) Arai, T.; Hu, Q.; Zheng, X.; Pu, L.; Sasai, H. *Org. Lett.* **2000**, *2*, 4261−4263. (c) Manickam, G.; Sundarajan, G. *Tetrahedron* **1999**, *55*, 2721−2736. (d) Sundararajan, G.; Prabagaran, N. *Org. Lett.* **2001**, *3*, 389−392. Zn·Li: (e) Nina, S.; Soai, K. *J. Chem. Soc., Perkin Trans. 1* **1991**, 2717−2720. Zn·Zn: (f) Trost, B. M.; Ito, H.; Silcoff, E. R. *J. Am. Chem. Soc.* **2001**, *123*, 3367−3368. (g) Yoshikawa, N.; Kumagai, N.; Matsunaga, S.; Moll, G.; Ohshima, T.; Suzuki, T.; Shibasaki, M. *J. Am. Chem. Soc.* **2001**, *123*, 2466−2467.

(4) (a) Ito, Y.; Sawamura, M.; Hayashi, T. *J. Am. Chem. Soc.* **1986**, *108*, 6405−6406. (b) Kitajima, H.; Ito, K.; Aoki, Y.; Katsuki, T. *Bull. Chem. Soc. Jpn.* **1997**, *70*, 207−217. (c) Sibi, M. P.; Cook, G. R.; Liu, P. *Tetrahedron Lett.* **1999**, *40*, 2477−2480. (d) Hamashima, Y.; Sawada, D.; Nogami, H.; Kanai, M.; Shibasaki, M. *Tetrahedron* **2001**, *57*, 805−814 and references therein. (e) Ooi, T.; Kondo, Y.; Maruoka, K. *Angew. Chem., Int. Ed. Engl.* **1997**, *36*, 1183−1185.

(5) For an application of this class of catalysts in the asymmetric Michael addition see: DiMauro, E. F.; Kozlowski, M. C. *Org. Lett.* **2001**, *3*, 1641−1644.

10.1021/om010571f CCC: $22.00
Publication on Web 02/28/2002

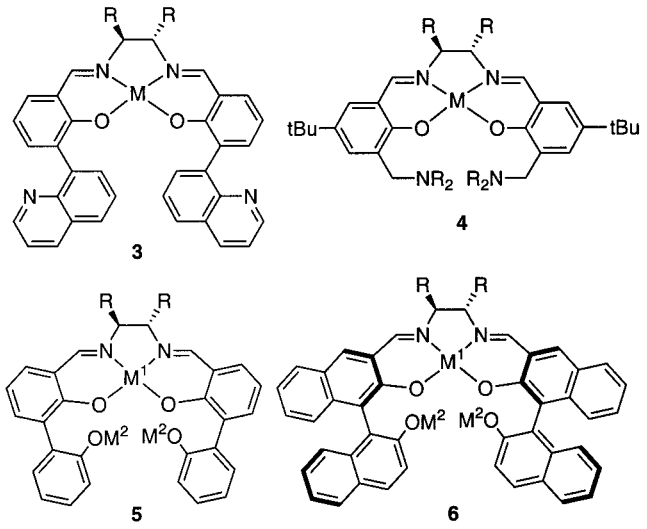

Figure 2.

heterobimetallic complexes **5** and **6** contain alkoxide bases.

Heterobimetallic bis(phenol)-salens **5** and **6** offer several advantages over complexes **3** and **4**. For example, the BINOL−salen allows variation in two metal centers: the Lewis acidic central metal and the alkali-metal naphthoxide counterion.[6] In addition, two chirality elements, the central chirality afforded by the diamine backbone and the axial chirality afforded by the biaryl portion, can be modified. The large number of known diamines and biphenol compounds allows the rapid construction of derivatives, facilitating optimization for a specific reaction as well as the delineation of the important structural features.

In this paper, the synthesis and structural characterization of the mixed salen−BINOL compound **6** are reported. From a comparison of the parent salen and the BINOL−salen (M^2 = H) crystallographic structures, the effect of the BINOL portions has been examined. In particular, the impact of intra- and intermolecular hydrogen bonding on the salen core structure has been analyzed.

Results and Discussion

Synthesis of the Ligands. The BINOL−salen ligands **8**−**10** needed to construct metal complexes of general structure **6** were prepared as shown in Scheme 1. Aldehyde **7**[7] was obtained from (*S*)-BINOL by lithiation and formylation of the bis-protected derivative. Cleavage of the MOM ethers then provided the precursor, which underwent ready condensation with various diamines to provide salens **8**−**10**. These novel ligands possess two chemically distinct sites—a salen portion and a pair of naphthol groups.

Synthesis of the Metal Complexes. A number of M^1-BINOL−salen complexes (**11**−**14**) incorporating Ni(II), Cu(II), Zn(II), or Pd(II) were prepared (eq 1). The

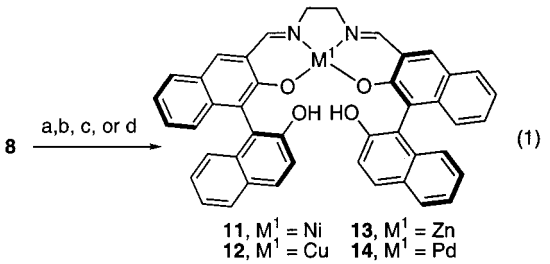

Ni(II) and Cu(II) complexes **11** and **12** were produced in a straightforward manner by treatment of the parent salen with the corresponding metal(II) acetate in refluxing EtOH. The resultant metal salen complexes were isolated by recrystallization. Formation of the Pd(II) complex **12** first required deprotonation of the salen with NaOMe. Treatment of the resultant dianion with $Pd(OAc)_2$ then provided the Pd(II) complex, which could also be crystallized. Application of a similar protocol to form the Pt(II) complex using $PtCl_2$ was not successful. The Zn(II) complex is expected to be hydrolytically unstable and was not isolated. Rather, the salen was treated with Et_2Zn at room temperature to generate the Zn(II) complex **13** in situ**.**

The diastereomeric Ni(II) and Cu(II) complexes derived from the diaminocyclohexane−BINOL−salen ligands **9** and **10** were prepared analogously, as shown in Scheme 2. The metal complexes were readily isolated in pure form by precipitation.

Structure of the Metal Complexes. The late transition metals nickel, copper, zinc, and palladium were selected for M^1 on the basis of their affinity for nitrogen, to promote the salen binding mode over an undesired mode involving coordination to only the BINOL components (Figure 3). Consistent with formation of the desired complexes, a lower C=N stretch in the IR spectra of the complexes relative to that of the free salen was observed. Also, a C_2 symmetry element is indicated from the ^{13}C NMR spectrum of the Ni− and Pd−BINOL−salen complexes. An X-ray crystal structure

Scheme 1

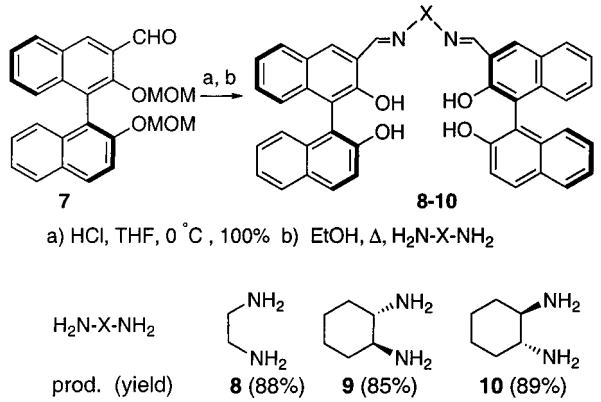

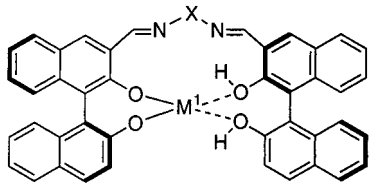

Figure 3. Undesired metal binding mode in the BINOL−salens.

(6) For a review of binaphthyl-derived catalysts see: Pu, L. *Chem. Rev.* **1998**, *98*, 2405−2494.

(7) Matsunaga, S.; Das, J.; Roels, J.; Vogl, E. M.; Yamamoto, N.; Iida, T.; Yamaguchi, K.; Shibasaki, M. *J. Am. Chem. Soc.* **2000**, *122*, 2252−2260.

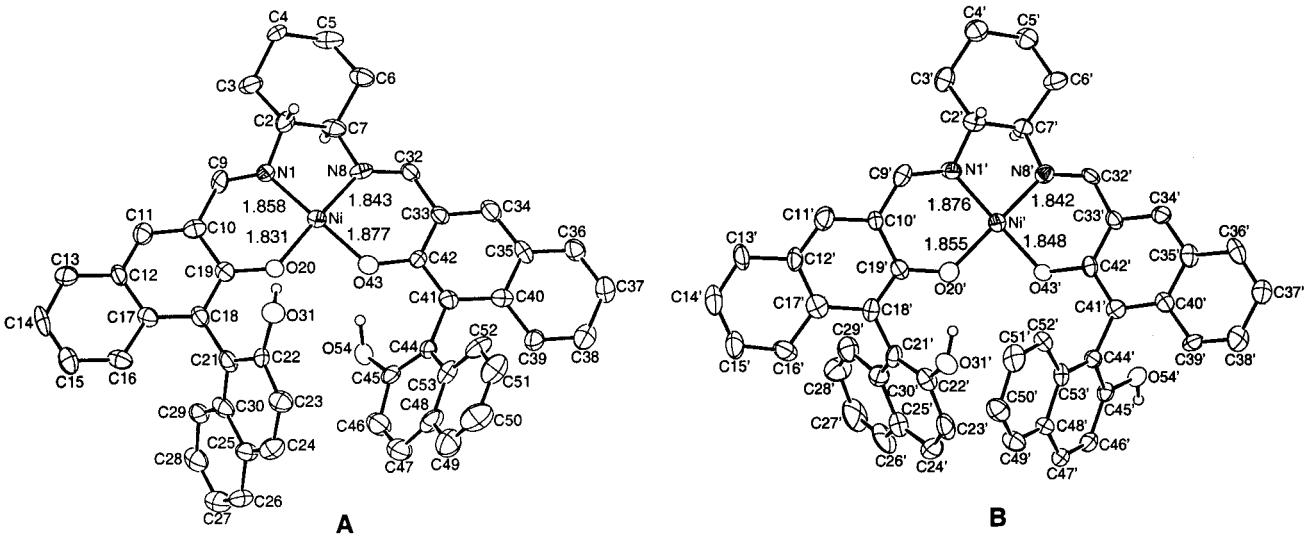

Figure 4. ORTEP diagram of the two structures found in the unit cell of **17**. Thermal ellipsoids are at the 30% probability level. Non-heteroatom hydrogens are omitted for clarity.

Scheme 2

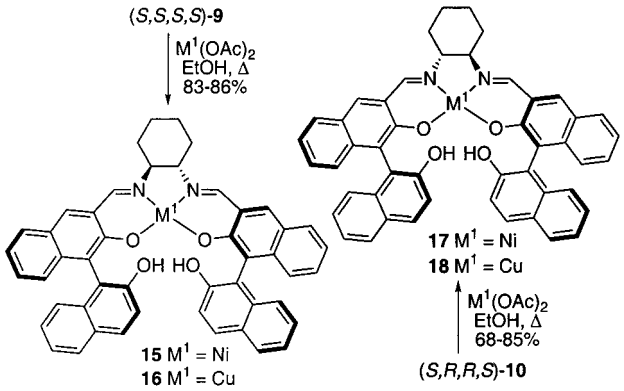

of the nickel complex (*S*,*R*,*R*,*S*)-**17** provided further evidence for the salen coordination motif.[8]

Two conformational forms of the salen were observed in the unit cell, as illustrated in Figure 4. Selected parameters are shown in Tables 1 and 2. These structures differ with respect to the orientation of one of the ancillary naphthol rings with respect to the plane of the salen. In structure **17-A**, the ancillary naphthols adopt a parallel arrangement with one naphthoate oxygen above the plane and one below the plane of the salen. The hydrogens on these naphthols hydrogen bond with the metal-bound oxygen of each BINOL fragment. As such, each salen oxygen is participating in one intramolecular hydrogen bond.

In the second complex (**B**) in the unit cell, the ancillary naphthols adopt a nonparallel arrangement, while most of the other features are the same as the first structure. Once again, one naphthoate oxygen is above the plane and one below the plane of the salen; however, only one of the naphthols forms an intramolecular hydrogen bond with the salen nucleus. The second naphthol participates in an intermolecular hydrogen bond with a naphthoate oxygen from the other complex (**A**) in the unit cell. The overall hydrogen bonding pattern is outlined schematically in Figure 5.

(8) Crystal data for **17**: $NiC_{49}H_{38}N_2O_4Cl_6$, formula weight 990.22, monoclinic, $P2_1$ (No. 4), a = 14.9158(5) Å, b = 17.2044(8) Å, c = 18.3523(6) Å, β = 97.040(3)°, V = 4674.0(3) Å^3, Z = 4, D_{calcd} = 1.407 g/cm^3, T = 200 K, μ(Mo Kα) = 8.04 cm^{-1}, R1 (wR2) = 0.0948 (0.2276), crystal dimensions 0.42 × 0.10 × 0.03 mm. The intensity data were corrected for Lorentz and polarization effects but not for absorption. The structure was solved by direct methods and refined by full-matrix least-squares methods. The asymmetric unit includes six disordered CH_2Cl_2 solvent molecules. The data were corrected for the presence of disordered solvent using SQUEEZE. Non-hydrogen atoms were refined anisotropically, and hydrogen atoms were refined using a "riding" model.

Table 1. Selected Bond Distances (Å), Bond Angles (deg), and Dihedral Angles (deg) for 17 and 19

	Compound **17**	
	17-A	**17-B**
Ni−N1	1.858(8)	1.876(8)
Ni−N8	1.843(8)	1.842(8)
Ni−O20	1.831(6)	1.855(7)
Ni−O43	1.877(7)	1.848(6)
O20−C19	1.327(11)	1.324(11)
O31−C22	1.382(11)	1.307(13)
O43−C42	1.329(10)	1.345(10)
O54−C45	1.375 (12)	1.355(11)
N1−Ni−N8	86.9(3)	85.0(3)
N1−Ni−O20	95.2(3)	94.8(3)
N8−Ni−O43	93.9(3)	94.3(3)
O20−Ni−O43	84.0(3)	86.9(3)
N1−Ni−O43	177.8(3)	173.3(3)
N8−Ni−O20	177.3(3)	171.0(3)
C17−C18−C21−C22	−119.1(1.0)	−119.02(1.09)
C17−C18−C21−C30	64.1(1.2)	59.9(1.3)
C19−C18−C21−C22	53.0(1.2)	60.7(1.3)
C19−C18−C21−C30	−123.9(1.0)	−120.4(1.0)
C40−C41−C44−C45	−120.8(0.9)	−76.7(1.1)
C40−C41−C44−C53	55.2(1.1)	97.6(1.0)
C42−C41−C44−C45	56.3(1.1)	103.2(1.0)
C42−C41−C44−C53	−127.7(0.9)	−82.5(1.1)

	Compound **19**		
Ni−N1	1.850(3)	Ni−O1	1.850(3)
Ni−N2	1.850(3)	Ni−O2	1.851(3)
N1−Ni−N2	86.3(1)	O1−Ni−O2	85.5(1)
N1−Ni−O1	94.6(1)	N1−Ni−O2	178.6(1)
N2−Ni−O2	93.8(1)	N2−Ni−O1	178.5(1)

Table 2. Hydrogen-Bonding Distances (Å) and Angles (deg) in 17

O20−O31	2.64	O20′−O31′	2.68
O43−O54	2.59	O54′−O54	2.65
C45−O54−O43	92.4	C22′−O31′−O20′	88.3
C22−O31−O20	89.9	C45′−O54′−O54	30.1

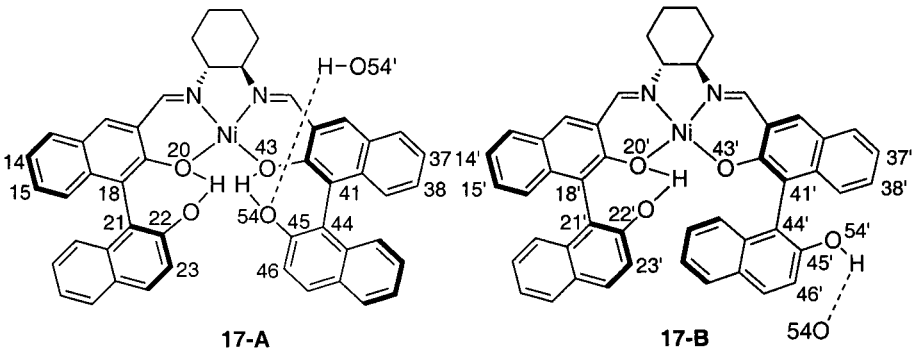

Figure 5.

The hydrogen-bonding arrangement in **17-A** introduces some strain, as indicated by the compressed binaphthyl dihedral angles of 63.2(1)° (for the C41−C44 biaryl) and 64.7(2)° (for the C18−C21 biaryl) in **17-A** when compared to the 78.3° biaryl dihedral of BINOL.[9] This strain also distorts the naphthols slightly out of plane near the point of oxygenation (Figure 6). Consistent with this analysis, the naphthol in **17-B** that does not participate in such an intramolecular hydrogen bond does not possess a similar distortion. In fact, the biaryl dihedral angle of 80.1(1)° for the C41′−C44′ biaryl is very close to that found in BINOL (78.3°). The naphthol in **17-B** participating in an intramolecular hydrogen bond is bent similarly to those in **17-A**, as reflected in the C18′−C21′ biaryl dihedral angle of 65.7(2)°.

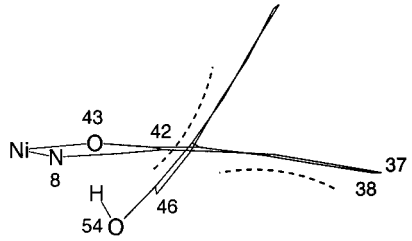

Figure 6. Line drawing of a projection along the C41−C44 biaryl bond from the X-ray structure, illustrating the distortion in one of the BINOL portions of **17-A**.

In **17-A**, the salen core, including the naphthyls that are conjugated to the imine, is relatively planar. The only exception is that the ends of the naphthyls furthest from the salen metal center curl away from the salen plane in a pseudo-C_2-symmetric manner. As illustrated in Figure 6, the naphthyl groups forming the salen core distort away from the nearer portion of the biaryl (as defined by a smaller average biaryl dihedral of 64°) and toward the more distant portion (as defined by a larger average dihedral of 116°). To minimize steric interactions and torsional strain, the imine hydrogens of **17-A** are forced above and below the plane of the salen anti to the axial hydrogens of the chiral cyclohexanediamine. This orientation reinforces the overall helical twist imposed onto the salen core by the BINOL portion (see Figure 6) and may account for the higher selectivity observed with catalysts derived from (*R*,*R*)-cyclohexanediamine and (*S*)-BINOL, the matched case (see below). Alternatively, the orientation of the axial hydrogens of the cyclohexanediamine may play a key role in defining the steric environment of the salen Lewis acid center and the naphthoxide base.

The presence of the two isomeric forms in the X-ray crystal structure permits examination of the consequences of hydrogen bonding on the structure and potentially the role of metal bridging on the reactivity of the salen metal portion. In the simple nickel salen structure **19**[10,11] (Figure 7), the nickel−heteroatom bonds are practically identical (1.850 Å). Comparison of this structure to **17-A** and **17-B** reveals that the metal−heteroatom bond distances are distorted from the ideal lengths seen in **19**.

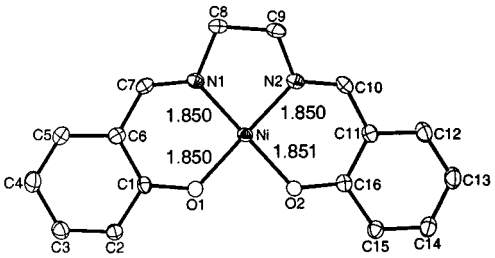

Figure 7. ORTEP diagram of **19**. Thermal ellipsoids are at the 30% probability level.

In isomer **17-A**, the bond distance (1.877 Å) between nickel and salen oxygen O43, which is part of a two-hydrogen-bond array (O43−O54−O54′), is longer than the bond distance (1.831 Å) between nickel and salen oxygen O20, which participates in only one hydrogen bond. This analysis is consistent with less electron density at O43, due to diffusion through the larger hydrogen-bonding network. Similarly, in **17-B** the bond distance (1.855 Å) between nickel and salen oxygen O20′, which is part of a one-hydrogen-bond array, is longer than the bond distance (1.848 Å) between nickel and salen oxygen O43′, which does not participate in any hydrogen bonds. While the explanation for the Ni−O bond lengths is consistent within each structure, the overall ranking of the bond lengths and comparison to those in structure **19** is not consistent with an

(9) Toda, F.; Tanaka, K.; Miyamoto, H.; Koshima, H.; Miyahara, I.; Hirotsu, K. *J. Chem. Soc., Perkin Trans. 2* **1997**, 1877−1885.

(10) Crystal data for **19**: $NiC_{16}H_{14}N_2O_2$, formula weight 325.00, orthorhombic, *Pbca* (No. 61), $a = 7.42900(10)$ Å, $b = 13.7402(2)$ Å, $c = 26.0687(4)$ Å, $V = 2660.99(7)$ Å^3, $Z = 8$, $D_{calcd} = 1.622$ g/cm^3, $T = 200$ K, μ(Mo Kα) = 14.63 cm^{-1}, R1 (wR2) = 0.0629 (0.1198), crystal dimensions 0.48 × 0.45 × 0.01 mm. The intensity data were corrected for Lorentz and polarization effects but not for absorption. The structure was solved by direct methods and refined by full-matrix least-squares methods. Non-hydrogen atoms were refined anisotropically, and hydrogen atoms were refined isotropically.

(11) The X-ray structure of **19** has been reported previously at lower resolution: (a) Shjik'nikova, L. M.; Yumal', E. M.; Shugam, E. A.; Voblikova, V. A. *Zh. Struct. Khim.* **1970**, *11*, 886−890. (b) Gourdon, A.; Prout, K. *Acta Crystallogr., Sect. C* **1983**, *39*, 865−868.

analysis in which a greater number of hydrogen-bond interactions leads to weaker Ni−O interactions. Since the variations in bond lengths are relatively small, these hydrogen bonds are likely weak, which is also consistent with the presence of two hydrogen-bonding patterns.

Replacement of the two hydrogens in complex **17** with Li, Na, K, or Cs would provide metal complexes containing Lewis acidic and basic sites. From the above analysis of the protonated form, interactions between the naphthoate cation and the salen oxygens are likely weak in these complexes. As a result, it should be possible to modulate the reactivity of the salen Lewis acid and the naphthoate base independently.

Application of the Metal Complexes. An edge view of the X-ray crystal structure of **17-A** (Figure 8) illustrates the nonplanar arrangement of the BINOL naphthyl rings. The remaining phenol groups cannot coordinate the salen metal center directly but are located nearby and may direct a latent nucleophile to an electrophile activated by the salen metal center.

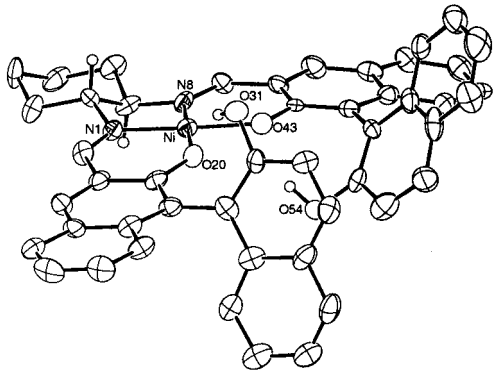

Figure 8. Edge-on ORTEP diagram of **17-A** illustrating the orientation of the biaryl rings.

To test for this type of reactivity, the BINOL−salen metal complexes were examined in the Michael reaction[5,12] of cyclohexenone with benzyl malonate (Table 2). The active catalysts, **20a**−**l**, were generated from the preformed M[1]−BINOL−salen complexes **11**−**18** via treatment with the indicated base in THF[13] prior to addition of the reaction substrates (eqs 2 and 3).

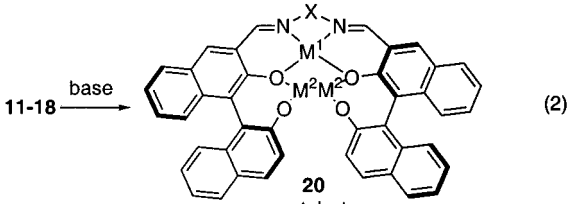

(2)

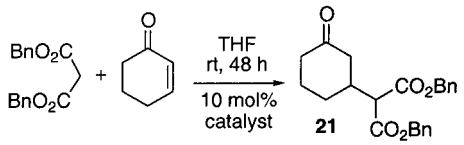

(3)

(12) For recent reviews, see: (a) *Comprehensive Asymmetric Catalysis*; Jacobsen, E. N., Pfaltz, A., Yamamoto, H., Eds.; Springer: New York, 1999; Chapter 31. (b) Leonard, J.; Ciez-Barra, E.; Merino, S. *Eur. J. Org. Chem.* **1998**, 2051−2061.

(13) Of the solvents examined with the Ni·Cs−BINOL−salen catalyst **20d** (toluene, THF, CH_2Cl_2, CH_3CN, DMF), THF gave the best results.

Table 3. Salen−Naphthoxide Complexes (Eq 2) in the Michael Addition Reaction (Eq 3)

entry	ligand	catalyst	M^1	M^2	base	% yield[a]	% ee[b]
1	**8**	**11**	Ni	H		0	
2[c]	**8**	**20a**	Ni	Li	LiH	63	11 (*S*)
3[c]	**8**	**20b**	Ni	Na	NaH	56	13 (*R*)
4[c]	**8**	**20c**	Ni	K	KH	70	10 (*R*)
5	**8**	**20a**	Ni	Li	LiOtBu	20	2 (*S*)
6	**8**	**20b**	Ni	Na	NaOtBu	55	7 (*R*)
7	**8**	**20c**	Ni	K	KOtBu	75	15 (*R*)
8	**8**	**20c**	Ni	K	K_3PO_4	20	44 (*R*)
9	**8**	**20c**	Ni	K	K_2CO_3	<5	
10	**8**	**20d**	Ni	Cs	Cs_2CO_3	80	31 (*R*)
11	**8**	**20h**	Cu	Cs	Cs_2CO_3	73	31 (*R*)
12	**8**	**20i**	Zn	Cs	Cs_2CO_3	57	8 (*R*)
13	**8**	**20j**	Pd	Cs	Cs_2CO_3	70	10 (*R*)
14	**9**	**20k**	Ni	Cs	Cs_2CO_3	84	54 (*R*)
15	**10**	**20l**	Ni	Cs	Cs_2CO_3	79	71 (*R*)
16	**10**	**20l**	Ni	Cs	Cs_2CO_3	56	87 (*R*)[d]
17	**10**	**20l**	Ni	Cs	Cs_2CO_3	45	90 (*R*)[e]

[a] Isolated yields. [b] Enantiomeric excess determined by HPLC. Absolute configuration based on optical rotation values. [c] 20 mol % catalyst. [d] At −20 °C for 5 days. [e] At −40 °C for 5 days.

Beginning with Ni(II)−salen complex **11**, the effects of M^2 were examined (entries 1−10, Table 3). Upon close examination of the results, a correlation between increased enantioselectivity and increased atomic radius/polarizability of M^2 is evident. Overall, use of Cs_2CO_3 as the base was optimal, providing high reactivity and some selectivity. The role of the base counterion (H^-, tBuO$^-$, $K_2PO_4^-$, KCO_3^-, $CsCO_3^-$) is obviously important but remains unclear. With both the Ni·M^2−BINOL−salen and Cu·M^2−BINOL−salen catalysts, switching M^2 from Li to Na results in a reversal in facial selectivity.[1d,14]

Replacement of both phenolic protons with a divalent metal (M^1:M^2 = 1:1) such as Zn, Mg, or Ca provided metal complexes (eq 4) which were catalytically inactive. Presumably, a stable tetrahedral complex forms between the four BINOL oxygens, rendering the naphthoates ineffective as bases (eq 4).

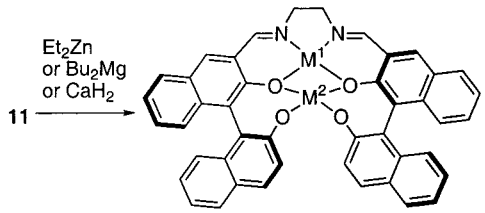

(4)

20e M^2 = Zn, **20f** M^2 = Mg, **20g** M^2 = Ca

Next, the effects of M^1 were examined with M^2 = Cs held constant (entries 10−13). The Cu catalyst **20h** was found to be almost as effective as the Ni derivative **20d**, while the Zn catalyst **20i** was slightly less reactive and substantially less selective. In an important control experiment, the Pd catalyst **20j** was found to be as reactive as the corresponding Ni catalyst **20d** but much less selective. The Pd(II) derivative is expected to be geometrically similar to the Ni derivative but less Lewis acidic. The lower selectivity for the Pd catalyst **20j** indicates that the Lewis acidity of the salen metal center is important to the stereochemical course of the reaction, as expected if the salen metal center serves to activate the cyclohexenone electrophile. Among the various

(14) A similar phenomenon has been observed for the La-linked BINOL catalyst of Shibasaki.[1d]

metal combinations examined, the Ni·Cs−BINOL−salen catalyst **20d** provided the best result (entry 10).

The *trans*-diaminocyclohexane Ni·Cs catalysts **20k** and **20l**, derived from the diastereomeric Ni−BINOL−salen complexes **15** and **17**, respectively, were also examined (Table 3, entries 14 and 15). Presumably one of these derivatives contains "matched" chirality elements, wherein the BINOL ligand reinforces the helical twist of the salen created by the cyclohexanediamine, while the other contains "mismatched" chirality elements. The catalyst derived from (*R*,*R*)-cyclohexanediamine and (*S*)-BINOL proved to be the matched catalyst system, providing the Michael adduct in 71% ee. Contrary to expectations, both of the Ni·Cs−BINOL−salen catalysts derived from **15** and **17** catalyzed the reaction with improved selectivity over that of ethylenediamine Ni·Cs−BINOL−salen catalyst (**20d**) derived from complex **11**. Since catalysts differing only in the configuration of the bis(imine) backbone afforded the same prevailing enantiomer in the product, the chirality in the biaryl axis appears to be the dominant control element responsible for facial selectivity. When the reaction mixture is cooled to −40 °C, the Michael adduct is obtained in up to 90% ee with 10 mol % **20l** (entry 17).

Conclusions

Late-transition-metal complexes of salens incorporating two chiral BINOL moieties have been synthesized and characterized crystallographically. The corresponding bis(naphthoxide) complexes have been found to catalyze the asymmetric addition of benzyl malonate to cyclohexenone in up to 90% ee. With these highly modular catalysts, the components controlling electrophilic and nucleophilic activation of substrates can be independently altered.

Experimental Section

General Considerations. Unless otherwise noted, all nonaqueous reactions were carried out under an atmosphere of dry N_2 in dried glassware. When necessary, solvents and reagents were dried prior to use. Toluene and CH_2Cl_2 were deoxygenated by purging with N_2 and then dried by passing through activated alumina. CH_3CN and EtOH were distilled from CaH_2. DMF was distilled from $MgSO_4$. TMEDA was distilled from Na. THF used in the catalytic Michael reactions was distilled from Na/benzophenone ketyl. $Ni(OAc)_2·4H_2O$, $Cu(OAc)_2$, and $Pd(OAc)_2$ were purchased from Strem and were used without further purification. Cyclohexenone and benzyl malonate were purchased from Aldrich, and cyclohexenone was distilled prior to use. $ZnEt_2$ was used as a freshly prepared 1 M solution in toluene. NaO^tBu, KO^tBu, LiO^tBu, and Cs_2CO_3 were dried with gentle heating under high vacuum and stored in the glovebox. All salen complexes were dried thoroughly with gentle heating under high vacuum for several hours prior to use. 2,2′-Bis((methoxymethyl)oxy)-1,1′-binaphthalene-3-carboxaldehyde,[7] (−)-(1*R*,2*R*)-cyclohexanediamine, and (+)-(1*S*,2*S*)-cyclohexanediamine were prepared according to established procedures.[15]

Analytical thin-layer chromatography (TLC) was performed on EM Reagents 0.25 mm silica gel 60-F plates. Preparative thin-layer chromatography was performed on EM Reagents 1.00 mm silica gel plates. Visualization was accomplished with UV light. Chromatography on silica gel was performed using a forced flow of the indicated solvent system on EM Reagents silica gel 60 (230−400 mesh).[16] Analytical high-performance liquid chromatography (HPLC) was performed on a Waters 600 HPLC with UV detection at 254 nm. Analytical Chiralpak AD and Chiralpak AS columns (0.46 cm × 25 cm) from Daicel were used. ^1H NMR spectra were recorded on Bruker AM-500 (500 MHz), AM-250 (250 MHz), or AM-200 (200 MHz) spectrometers. Chemical shifts are reported in ppm from tetramethylsilane (0 ppm) or from the solvent resonance ($CDCl_3$, 7.26 ppm; DMSO-d_6, 2.49 ppm; D_2O, 4.80 ppm). Data are reported as follows: chemical shift, multiplicity (s = singlet, d = doublet, t = triplet, q = quartet, br = broad, m = multiplet), coupling constants, and number of protons. Mass spectra were obtained on a low-resonance Micromass Platform LC in electron spray mode and high-resonance VG Autospec with an ionization mode of either CI or ES. IR spectra were taken on a Perkin-Elmer FT-IR spectrometer using a thin film on NaCl plates. Melting points were obtained on a Thomas Scientific Unimelt apparatus and are uncorrected. Optical rotations were measured on a Perkin-Elmer 341 polarimeter with a sodium lamp and are reported as follows: $[\alpha]^T_\lambda$ (c = g/100 mL, solvent).

(−)-(*S*)-1,1′-Binaphthalene-3-carboxaldehyde. Concentrated HCl (44 mL of a 12 M solution) was added dropwise to a solution of (−)-(*S*)-2,2′-bis((methoxymethyl)oxy)-1,1′-binaphthalene-3-carboxyaldehyde (4.0 g, 9.94 mmol) in THF cooled to 0 °C. After it was stirred for 3 h at room temperature, the solution was extracted with EtOAc and washed with water, saturated $NaHCO_3$, and brine. After drying over Na_2SO_4 and removal of solvent the diol was obtained in quantitative yield (3.12 g, 9.94 mmol) as a yellow solid: mp 208−210 °C; $[\alpha]^{20}_D$ −58 (*c* 1.0, $CHCl_3$); ^1H NMR (500 MHz, $CDCl_3$) δ 10.63 (br s, 1H), 10.19 (s, 1H), 8.36 (s, 1H), 8.02 (d, J = 8.9 Hz, 1H), 7.92 (d, J = 8.9 Hz, 1H), 7.82 (d, J = 8.14 Hz, 1H), 7.4−7.15 (m, 11 Hz), 7.1 (d, J = Hz, 1H), 4.9 (br s, 1H); ^{13}C NMR (125 MHz, $CDCl_3$) δ 151.4 (C═O), 139.1, 137.0, 133.3, 131.2, 130.5, 130.0, 129.3, 128.3, 127.8, 126.7, 125.1, 124.9, 124.4, 123.5, 122.2, 117.7; IR (film) 3417 (br), 2357, 1651 (C═O), 1504, 1386, 1338 cm^{-1}.

General Procedure for Preparation of BINOL−salens 8−10. (−)-(*S*)-1,1′-Binaphthalene-3-carboxaldehyde (2.0 equiv) was dissolved completely in EtOH (4 mL) with heating. The yellow solution was then cooled to room temperature, and the appropriate diamine (1.0 equiv) was added dropwise. During this addition, the product precipitated out of solution. The slurry was then stirred at room temperature for at least 24 h or with intermittent heating and cooling for approximately 12 h. The precipitate was collected by filtration, washed with cold EtOH, and dried with gentle heating in vacuo to provide the product.

(15) (a) Galsbol, F.; Steenbol, P.; Sondergaard Sorensen, B. *Acta Chem. Scand.* **1972**, *26*, 3605−3611. (b) Larrow, J. F.; Jacobsen, E. N.; Gao, Y.; Hong, Y.; Nie, X.; Zepp, C. M. *J. Org. Chem.* **1994**, *59*, 1939−1942.

(16) Still, W. C.; Kahn, M.; Mitra, A. *J. Org. Chem.* **1978**, *43*, 2923−2925.

(−)-(*S,S*)-Ethylenediamine−BINOL−salen (8). Using the general procedure with ethylenediamine provided **8** in 88% yield (275 mg, 0.421 mmol) as a pale orange powder: mp 183−186 °C; $[\alpha]^{20}_D$ −95 (*c* 1.0, $CHCl_3$); ^{1}H NMR (500 MHz, $CDCl_3$) δ 13.3 (br s, 2H), 8.59 (s, 2H, HC═N), 7.85 (m, 8H), 7.4−7.0 (m, 14H), 5.05 (br s, 2H), 3.95 (m, 4H, H_2C−N); ^{13}C NMR (125 MHz, $CDCl_3$) δ 166.7 (C═N), 155.4, 151.5, 135.3, 134.7, 133.5, 130.0, 129.2, 129.0, 128.9, 128.2, 127.6, 126.4, 124.7, 124.6, 123.9, 123.2, 120.6, 117.7, 59.4 (C−N); IR (film) 3423 (br), 2358, 1647 (C═N), 1506, 1339 cm^{-1}; MS (ES) *m/z* 653 (MH^+), 675 (MNa^+), 676 ($MHNa^+$).

(−)-(*S,S,S,S*)-Diaminocyclohexane−BINOL−salen (9). Using the general procedure with (+)-(1*S*,2*S*)-diaminocyclohexane provided **9** in 85% yield: mp 193−196 °C; $[\alpha]^{20}_D$ +270 (*c* 0.5, $CHCl_3$); ^{1}H NMR (500 MHz, $CDCl_3$) δ 13.52 (br s, 2H), 8.52 (s, 2H, HC═N), 7.97 (d, *J* = 8.9 Hz, 2H), 7.92 (d, *J* = 8.1 Hz, 2H), 7.87 (s, 2H), 7.81 (d, *J* = 7.7 Hz, 2H), 7.42 (d, *J* = 8.9 Hz, 2H), 7.36−7.29 (m, 6H), 7.15 (d, *J* = 8.1 Hz, 2H), 7.07 (d, *J* = 8.4 Hz, 2H), 5.11 (br s, 2H), 3.38 (d, *J* = 8.9 Hz, 2H) (HC−N), 2.0 (d, *J* = 13.4 Hz, 2H), 1.9 (d, *J* = 9.3 Hz, 2H), 1.74 (d, *J* = 9.3 Hz, 2H), 1.47 (t, *J* = 10.2 Hz, 2H); ^{13}C NMR (125 MHz, $CDCl_3$) δ 165.3 (C═N), 155.9, 151.8, 135.6, 135.0, 133.9, 130.5, 129.7, 129.6, 129.5, 128.7, 128.1, 126.9, 125.1, 125.0, 124.3, 123.7, 121.0, 118.1, 114.8, 113.7, 73.3 (C−N), 33.2, 24.4; IR (film) 3507 (br), 3423 (br), 3057, 2933, 2859, 1631 (C═N), 1510, 1344 cm^{-1}; MS (ES) *m/z* 729 (MNa^+); HRMS (ES) calcd *m/z* 707.290 983 ($C_{48}H_{39}N_2O_4$, MH^+), found *m/z* 707.290 854.

(−)-(*S,R,R,S*)-Diaminocyclohexane−BINOL−salen (10). Using the general procedure with (−)-(1*R*,2*R*)-diaminocyclohexane provided **10** in 89% yield: mp 185−188 °C; $[\alpha]^{20}_D$ −342 (*c* 0.5, $CHCl_3$); ^{1}H NMR (500 MHz, $CDCl_3$) δ 13.43 (br s, 2H), 8.56 (s, 2H, C═N), 7.90 (m, 8H), 7.37−7.10 (m, 14H), 5.05 (br s, 2H), 3.36 (m, 2H) (CH−N), 2.0−1.43 (m, 8H); ^{13}C NMR (125 MHz, $CDCl_3$) δ 165.0 (C═N), 155.5, 151.5, 135.3, 134.7, 133.5, 130.0, 129.3, 129.2, 129.0, 128.2, 127.8, 126.5, 124.8, 124.6, 123.9, 123.3, 120.6, 117.7, 114.4, 113.4, 72.2 (C−N), 32.7, 24.1; IR (film) 3414 (br), 3055, 2931, 2858, 1628 (C═N), 1506, 1344 cm^{-1}; MS (ES) *m/z* 729 (MNa^+), 747 (M − CH_3CN^+); HRMS (ES) calcd *m/z* 707.2910 ($C_{48}H_{39}N_2O_4$, MH^+), found *m/z* 707.2913.

(−)-(*S,S*)-Ni(II)−Ethylenediamine−BINOL−salen (11). Two methods could be used interchangeably.

Method A. BINOL−salen **8** (100 mg, 0.153 mmol) and $Ni(OAc)_2 \cdot 4H_2O$ (27 mg, 0.153 mmol) were combined in a flask with EtOH (3 mL). After the mixture was heated at reflux for 1 h, the dark yellow slurry became dark orange. The mixture was cooled slowly to room temperature and then stored at 0 °C for 1 h. The fine red precipitate was collected by vacuum filtration, washed with cold EtOH, and dried in vacuo with gentle heating for several hours to provide **11** in 65% yield (70 mg, 0.099 mmol) as a red solid.

Method B. (−)-(*S*)-1,1′-Binaphthalene-3-carboxaldehyde (105 mg, 0.33 mmol) was dissolved completely in EtOH (3 mL) with heating. The yellow solution was then cooled to room temperature, and ethylenediamine (11 μL, 0.17 mmol) was added dropwise. During this addition, the product precipitated out of solution. The pale orange slurry was then stirred at room temperature for 24 h. $Ni(OAc)_2 \cdot 4H_2O$ (31 mg, 0.17 mmol) was added, and the slurry was heated at reflux for 2 h and then cooled slowly to room temperature and stored at 0 °C for 1 h. The fine red precipitate was collected by vacuum filtration and washed with cold EtOH and then dried in vacuo with gentle heating for several hours to provide **11** in 68% yield (80 mg, 0.11 mmol): mp >300 °C dec; ^{1}H NMR (500 MHz, CD_2Cl_2) δ 8.0 (d, *J* = 8.1 Hz, 2H), 7.84−7.79 (m, 6H), 7.69 (d, *J* = 7.7 Hz, 2H), 7.37 (t, *J* = 7.5 Hz, 2H), 7.22 (t, *J* = 7.5 Hz, 2H), 7.12−7.05 (m, 5H), 6.6 (m, 3H), 6.47 (d, *J* = 8.7 Hz, 2H), 3.46 (dd, *J* = 38, 8 Hz, 4H); ^{13}C NMR (125 MHz, CD_2Cl_2) δ 164.7 (C═N), 156.3, 153.5, 137.9, 136.4, 134.3, 129.7, 129.5, 129.3, 128.8, 128.4, 126.3, 126.2, 125.8, 125.7, 124.1, 123.0, 122.5, 120.8, 118.3, 118.0, 59.4 (C−N); IR (film) 3429 (br), 1638 (C═N), 1512, 1427 cm^{-1}; MS (ES) *m/z* 731 (MNa^+), 749 (M − CH_3CN^+); HRMS (ES) calcd *m/z* 709.1637 ($C_{44}H_{31}N_2O_4Ni$, MH^+), found *m/z* 709.1629.

(−)-(*S,S*)-Cu(II)−Ethylenediamine−BINOL−salen (12). BINOL−salen **8** (300 mg, 0.459 mmol) and $Cu(OAc)_2$ (83.5 mg, 0.459 mmol) were combined in a flask with EtOH (11 mL) and water (1.1 mL). The mixture was heated at reflux for 2.5 h, stirred at room temperature for 1 h, and stored at 0 °C for 1 h. The fine brown precipitate was collected by gravity filtration, washed with Et_2O, and dried in vacuo with gentle heating for several hours to provide **12** in 92% yield (303 mg, 0.424 mmol) as a brown solid: mp >300 °C dec; IR (film) 3442.0 (br), 2368, 2338, 1640 (C═N), 1512, 1437 cm^{-1}; MS (ES) *m/z* 714 (MH^+); HRMS (ES) calcd *m/z* 714.157 982 ($C_{44}H_{31}N_2O_4Cu$, MH^+); found *m/z* 714.604 03.

(−)-(*S,S*)-Pd(II)−Ethylenediamine−BINOL−salen (14). BINOL−salen **8** (100 mg, 0.150 mmol) and MeONa (19.8 mg, 0.360 mmol) were combined in a flask with MeOH (11.5 mL). The orange solution was stirred at room temperature for 15 min, and $Pd(OAc)_2$ (33.7 mg, 0.150 mmol) was added at once. The orange-brown slurry was stirred for 3 h and then stored at 0 °C for 1 h. The precipitate was collected by vacuum filtration, washed with cold MeOH and then Et_2O, and dried in vacuo with gentle heating for several hours to provide **14** in 87% yield (99.1 mg, 0.131 mmol) as a brown-orange solid: mp >300 °C dec; ^{1}H NMR (500 MHz, DMSO-d_6) δ 8.60 (s, 2H), 8.21 (s, 2H), 7.92 (d, *J* = 8.6 Hz, 4H), 7.79 (d, *J* = 8.5 Hz, 4H), 7.22 (t, *J* = 7.4 Hz, 2H), 7.06 (m, 4H), 6.81 (d, *J* = 8.4 Hz, 2H), 6.70 (d, *J* = 8.8 Hz, 2H), 6.55 (d, *J* = 8.2 Hz, 2H), 3.99 (br s); ^{13}C NMR (125 MHz, THF-d_8) δ 161.4 (C═N), 156.9, 154.3, 138.0, 137.4, 134.6, 129.8, 129.3, 128.6, 128.3, 127.8, 126.5, 126.0, 125.9, 125.8, 125.3, 122.5, 121.3, 119.1, 118.7, 60.1; IR (film) 3499 (br), 3049, 2918, 1614 (C═N), 1580, 1344, 1310 cm^{-1}; MS (ES) *m/z* 779 (MNa^+); HRMS (ES) calcd *m/z* 779.1138 ($C_{44}H_{30}N_2O_4PdNa$, MNa^+); found *m/z* 779.1168.

(−)-(*S,S,S,S*)-Ni(II)−Diaminocyclohexane−BINOL−salen (15). Compound **15** was prepared from **9** in 83% yield following method A for the preparation of **11**: mp >300 °C dec; ^{1}H NMR (500 MHz, CD_2Cl_2) δ 8.06 (s, 2H), 7.99 (d, *J* = 8.0 Hz, 2H), 7.93 (s, 2H), 7.81 (d, *J* = 8.0 Hz, 2H), 7.68 (d, *J* = 8.7 Hz, 2H), 7.38 (t, *J* = 7.4 Hz, 2H), 7.20 (t, *J* = 7.4 Hz, 2H), 7.15−7.06 (m, 6H), 6.78 (br s, 2H), 6.58 (d, *J* = 8.6 Hz, 2H), 6.18 (d, *J* = 8.7 Hz, 2H), 3.31 (br s, 2H), 2.63 (d, *J* = 10.9 Hz, 2H), 2.05 (d, *J* = 8.3 Hz, 2H), 1.46 (m, 4H); ^{13}C NMR (125 MHz, CD_2Cl_2) δ 160.5 (C═N), 156.2, 153.2, 137.9, 136.8,

134.3, 129.6, 129.3, 129.2, 128.7, 128.4, 126.4, 126.2, 125.8, 125.7, 124.2, 123.0, 122.4, 120.5, 118.3, 118.0, 70.9 (C−N), 29.3, 24.6; IR (film) 3215 (br), 3052, 2930, 1612 (C═N), 1583, 1347, 1323 cm^{-1}; MS (ES) *m*/z 785 (MNa^+); HRMS (ES) calcd *m*/z 763.210 680 ($C_{48}H_{37}N_2O_4Ni$, MH^+), found 763.210 049.

(−)-(*S,S,S,S*)-Cu(II)−Diaminocyclohexane−BINOL−salen (16). Compound **16** was prepared from **9** in 86% yield following the procedure for **12**, except that the product was washed with cold EtOH instead of Et_2O: mp >300 °C dec; IR (film) 3472 (br), 3053, 2935, 1613 (C═N), 1582, 1348, 1324 cm^{-1}; MS (ES) *m*/*z* 790 (MNa^+); HRMS (ES) calcd *m*/*z* 768.202 959 ($C_{48}H_{37}N_2O_4Cu$, MH^+); found *m*/*z* 768.204 932.

(−)-(*S,R,R,S*)-Ni(II)−Diaminocyclohexane−BINOL−salen (17). Compound **17** was prepared from **10** in 85% yield following method A for the preparation of **11**. X-ray-quality crystals of **17** were grown in CH_2Cl_2 layered with hexanes: mp >300 °C dec; ^1H NMR (500 MHz, CD_2Cl_2) δ 8.03−7.78 (m, 10H), 7.36 (t, J = 8.0 Hz, 2H), 7.23 (t, J = 8.0 Hz, 2H), 7.12−7.06 (m, 4H), 6.64 (d, J = 8.7 Hz, 2H), 6.62 (d, J = 8.6 Hz, 2H), 6.32 (s, 2H), 3.22 (m, 2H), 2.60 (m, 2H), 2.04 (m, 2H), 1.45 (m, 2H); ^{13}C NMR (125 MHz, CD_2Cl_2) δ 160.5 (C═N), 156.6, 153.3, 138.0, 136.9, 134.4, 129.6, 129.3, 129.2, 128.7, 128.3, 126.3, 126.2, 125.7, 125.6, 124.2, 122.9, 122.3, 120.7, 118.0, 117.9, 70.6 (C−N), 29.3, 24.6; IR (film) 3427 (br), 3055, 2941, 2859, 1613 (C═N), 1584, 1347, 1323 cm^{-1}; MS (ES) *m*/*z* 785 (MNa^+); HRMS (ES) calcd *m*/*z* 785.192 625 ($C_{48}H_{36}N_2O_4NiNa$, MNa^+); found *m*/*z* 785.194 218. Anal. Calcd for $C_{48}H_{36}N_2O_4N\cdot 2.5H_2O$: C, 71.30; H, 5.11; N, 3.46. Found: C, 71.56; H, 4.86; N, 3.38.

(−)-(*S,R,R,S*)-Cu(II)−Diaminocyclohexane−BINOL−salen (18). Compound **18** was prepared from **10** in 85% yield following the procedure for the preparation of **16**: mp >300 °C dec; IR (film) 3438 (br), 3054, 2937, 2859, 1613 (C═N), 1582, 1348, 1319 cm^{-1}; MS (ES) *m*/*z* 768 (M^+), 791 (MNa^+); HRMS (ES) calcd *m*/*z* 768.204 932 ($C_{48}H_{37}N_2O_4Cu$, MH^+), found *m*/*z* 768.208 454, calcd *m*/*z* 790.186 877 ($C_{48}H_{36}N_2O_4CuNa$, MNa^+), found 790.185 549.

General Procedure for the Michael Reaction of Cyclohexenone and Benzyl Malonate. M[1]−BINOL−salen species **11**−**18** (0.028 mmol) and base (0.056 mmol) were combined in a 10 mL flask in an inert-atmosphere glovebox. After the flask was sealed, removed from the glovebox, and placed under N_2, THF (5 mL) was added. The mixture was stirred at room temperature for 2.5 h and then cooled to the reaction temperature as necessary. Cyclohexenone (0.282 mmol) and benzyl malonate (0.282 mmol) were successively added. After it was stirred for 48 h, the reaction mixture was quenched with H_2O, extracted with EtOAc, dried over $MgSO_4$, and concentrated. The Michael adduct was isolated from the crude residue by preparative TLC (SiO_2; 50% EtOAc/50% hexanes). ^1H NMR (500 MHz, $CDCl_3$), and ^{13}C NMR (125 MHz, $CDCl_3$) spectra for 3-[bis((benzyloxy)carbonyl)methyl]cyclohexanone (**21**) were identical with those previously reported.[17]

The enantiomeric purity of the Michael adduct was determined by HPLC: Daicel Chiralpak AS, 10% 2-propanol/hexane, 0.9 mL/min; $t_R(+)$ = 29 min, $t_R(-)$ = 38 min. The absolute configuration of **21** has been determined.[18]

Acknowledgment. Financial support was provided by the National Institutes of Health (Grant No. GM-59945) and Merck Research Laboratories. The invaluable assistance of Dr. Patrick Carroll in obtaining and analyzing the X-ray structures is gratefully acknowledged.

Supporting Information Available: Text giving full details of the crystallographic methods and tables giving X-ray data. This material is available free of charge via the Internet at http://pubs.acs.org.

OM010571F

(17) Kim, Y. S.; Matsunaga, S.; Das, J.; Sekine, A.; Ohshima, T.; Shibasaki, M. *J. Am. Chem. Soc.* **2000**, *122*, 6506−6507.

(18) Sasai, H.; Arai, T.; Satow, Y.; Houk, K. N.; Shibasaki, M. *J. Am. Chem. Soc.* **1995**, *117*, 6194−6198.